Catalytic Mechanisms

A Switchable Catalyst Duo for Acyl Transfer Proximity Catalysis and Regulation of Substrate Selectivity

Abir Goswami[+], Sudhakar Gaikwad[+], and Michael Schmittel*[a]

Abstract: Enzymes are encoded with a gamut of information to catalyze a highly selective transformation by selecting the proper reactants from an intricate mixture of constituents. Mimicking biological machinery, two switchable catalysts with differently sized cavities and allosteric control are conceived that allow complementary size-selective acyl transfer in an on/off manner by modulating the effective local concentration of the substrates. Selective activation of one of two catalysts in a mixture of reactants of similar reactivity enabled upregulation of the desired product.

Many metalloenzymes use the proximity effect to control precise docking of substrates thereby activating processes with astounding selectivity.[1,2] Inspired by such mode of action, chemists have designed fascinating catalysts and catalytic machinery for controlling rate and selectivity.[3,4] However, almost all of those prototypes were conceived as stand-alone molecular devices operating only as individuals. Enzymes, in contrast, do not need spatial isolation because each of them is encoded with highly specific information for their mode of action. Conversely, encrypting information into multiple switchable man-made catalysts for achieving selectivity in mixtures of similar substrates still represents a major challenge.[5] Indeed, only a handful of systems is known showing clear-cut ON/OFF regulation[6] or selectivity switching.[7] Even more difficult is control of selectivity when substrates of similar reactivity but different size need to be differentiated,[3b,5a] requiring proximity catalysis.[8] Herein, we describe the switchable catalysts **1** and **2** (Figure 1) that were reversibly toggled between four different states upon sequential addition/removal of copper(I) and iron(II) ions. Alike in natural machinery,[9] ON/OFF control of

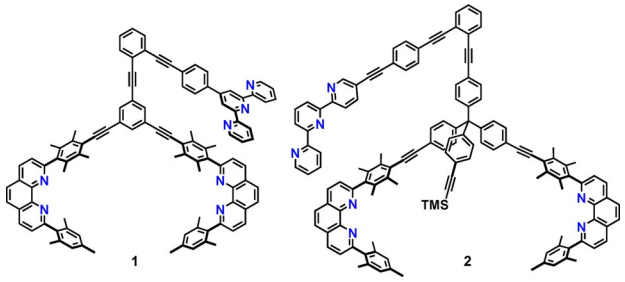

Figure 1. Chemical structures of nanoswitch **1** and **2**.

catalysis and substrate selectivity in acyl transfer reaction is possible by using allosteric effects[10] and by selectively activating only one catalyst in a mixture of two.

To pre-assess the proposed acyl transfer reaction (**A** + **B** → **C** + **D**),[11] we first prepared as model the *bis*-phenanthroline ligand **3** (Figure 2, for synthesis see Supporting Information, Scheme S2) to evaluate its potential for proximity catalysis. As reported earlier, sterically shielded phenanthrolines (phenAr_2) like **4** are kinetically impeded to form homoleptic complexes with copper(I) ions due to the bulk in 2- and 9-position and thus remain coordinatively frustrated in the form of [Cu(phen-Ar_2)]$^+$.[12] However, these copper(I) sites still allow HETeroleptic PYridine and Phenanthroline (HETPYP) type complexes[13] with

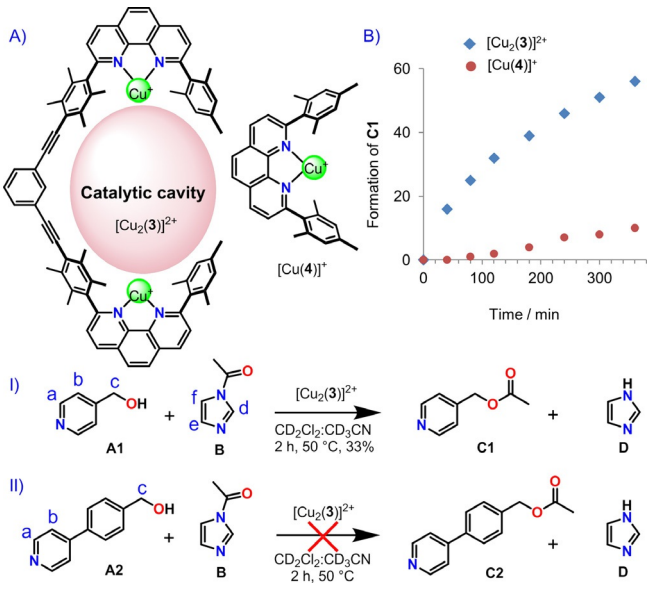

Figure 2. (A) Lewis-acid catalysis in the acyl transfer reactions I and II using model catalysts $[Cu_2(\mathbf{3})]^{2+}$ and $[Cu(\mathbf{4})]^+$. (B) Formation of **C1** in presence of $[Cu_2(\mathbf{3})]^{2+}$ and $[Cu(\mathbf{4})]^+$ as catalyst (50 °C).

[a] *Dr. A. Goswami,[+] Dr. S. Gaikwad,[+] Prof. Dr. M. Schmittel*
Center of Micro and Nanochemistry and Engineering, Organische Chemie I
University of Siegen
Adolf-Reichwein Str. 2, 57068 Siegen (Germany)
E-mail: schmittel@chemie.uni-siegen.de
[+] *These authors contributed equally to this work.*
Supporting information and the ORCID identification number(s) for the author(s) of this article can be found under: https://doi.org/10.1002/chem.202004416.

sterically undemanding monodentate ligands or substrates. Thus, substrates pyridin-4-yl-methanol (**A1**) and 1-acetylimidazole (**B**) were chosen that should weakly coordinate to the copper(I)-loaded phenAr$_2$ binding sites of ligands **3** and **4** (see Supporting Information, Figure S41).

The spatial arrangement of both copper(I) ions in $[Cu_2(\mathbf{3})]^{2+}$ was expected to pre-organize the substrates in close proximity within the cavity thus increasing their effective concentration. To test the catalytic activity of $[Cu_2(\mathbf{3})]^{2+}$, our chosen model, a mixture of ligand **3** (3 mM), $[Cu(CH_3CN)_4]PF_6$, reactants **A1** and **B** in a 1:2:10:10 ratio in CD_2Cl_2/CD_3CN (5:1, *v/v*) was heated at 50 °C for 2 h furnishing pyridin-4-ylmethyl acetate (**C1**) in 33% yield (Supporting Information, Figure S44). In the absence of $[Cu_2(\mathbf{3})]^{2+}$, under otherwise identical reaction conditions, no product formation was observed (Supporting Information, Figure S43). A further control experiment using the same set of conditions proved that 20 mol% of $[Cu(\mathbf{4})]^+$ was unable to afford any competitive amount of **C1** (in situ yield = 2%) (Supporting Information, Figure S45). Such finding suggested the existence of a proximity effect in the doubly copper(I)-loaded complex $[Cu_2(\mathbf{3})]^{2+}$.

To probe proximity catalysis in an ON/OFF manner, we decided to block and re-open one of the $[Cu(phenAr_2)]^+$ binding site by a competing stronger complexation such as the HETeroleptic Terpyridine And Phenanthroline (HETTAP) motif.[13] We thus designed nanoswitch **1** and implemented four distinct switching states by addition and removal of copper(I) and iron(II) ions (Figure 3).[14] Synthesis and characterization of nanoswitch **1** are detailed in the supporting information (Supporting Information, Scheme S1). When a solution of **1** in [D$_2$]dichloromethane was treated with one equiv of copper(I) ions, formation of the intramolecular complex $[Cu(\mathbf{1})]^+$ (= State I$_1$) was confirmed by ^{1}H NMR, ^{1}H-^{1}H COSY, electrospray ionization mass spectrum (ESI-MS), and elemental analysis. Two sets of phenanthroline signals (1:1, complexed vs. uncomplexed) in the ^{1}H NMR spectrum of $[Cu(\mathbf{1})]^+$ clearly indicated presence of an intramolecular HETTAP complex that desymmetrized both phenanthroline sites. The characteristic upfield shifted signal of the mesityl protons 9-H at the complexed phenAr$_2$ from 6.94 to 6.41 ppm due to shielding by the terpyridine unit attested the formation of $[Cu(\mathbf{1})]^+$. This assignment was further supported by the simultaneous upfield shift of the terpyridine proton signals for a-H and b-H from 8.66 and 7.28 ppm to 7.68 and 7.12 ppm, respectively (Supporting Information, Figure S22). The ESI-MS of the resultant complex displayed a molecular ion peak at $m/z = 1478.0$ that is diagnostic for the $[Cu(\mathbf{1})]^+$ due to the experimental isotopic splitting matching the computed one (Supporting Information, Figure S66).

Addition of one more equiv of copper(I) ions to the solution of State I$_1$ quantitatively furnished $[Cu_2(\mathbf{1})]^{2+}$ (= State II$_1$), where the additional equiv of copper(I) was bound at the second shielded phenanthroline site. The identity of the complex was corroborated by a correct elemental analysis and an ESI mass signal of the resulting complex $[Cu_2(\mathbf{1})]^{2+}$ (peak at $m/z = 770.1$, see SI, Figure S67). In the ^{1}H NMR, the HETTAP-free phenanthroline and its mesityl protons (9u-H) showed the anticipated downfield shifts in the ^{1}H NMR (Figure 4B, and Supporting Information, Figure S24). At room temperature, the two distinct sets of phenanthroline signals clearly indicated slow exchange of the terpyridine arm between both copper(I)-loaded phenanthrolines. A cross-correlation between proton 9c-H of the copper(I)-loaded phenanthroline (at 6.96 ppm) and proton 9-H of the HETTAP-complexed phenanthroline signal (at 6.38 ppm) in the ^{1}H-^{1}H ROESY experiment allowed measurement of the slow exchange.[15] The activation parameters for the exchange were determined at 298 K ($k = 1.34\ s^{-1}$ and $\Delta G^{\ddagger}_{298} = 72.6\ kJ\ mol^{-1}$) (Supporting Information, Figure S42).

Addition of iron(II) ions to State II$_1$ was expected to furnish a bishomoleptic complex at the tridentate terpyridine sites (State III$_1$ = $[FeCu_4(\mathbf{1})_2]^{6+}$).[16] Indeed, upon addition of 0.5 equiv of iron(II) ions to complex $[Cu_2(\mathbf{1})]^{2+}$, the HETTAP complex in $[Cu_2(\mathbf{1})]^{2+}$ was instantly cleaved to yield the bishomoleptic iron(II) complex $[FeCu_4(\mathbf{1})_2]^{6+}$ (State III$_1$), a quantitative transformation that could easily be followed by the naked eye (Figure 5A). The notable upfield shift of the terpyridine protons a-H from 7.69 to 7.13 ppm and b-H from 7.11 to 7.04 ppm unam-

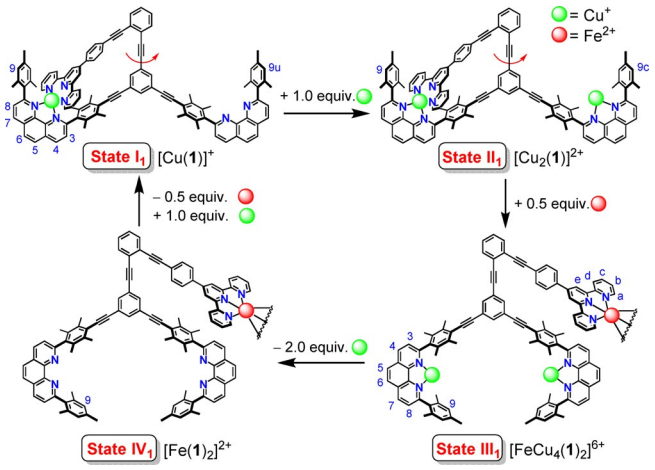

Figure 3. Four-state switching of nanoswitch **1** by addition/removal of copper(I) and iron(II) ions.

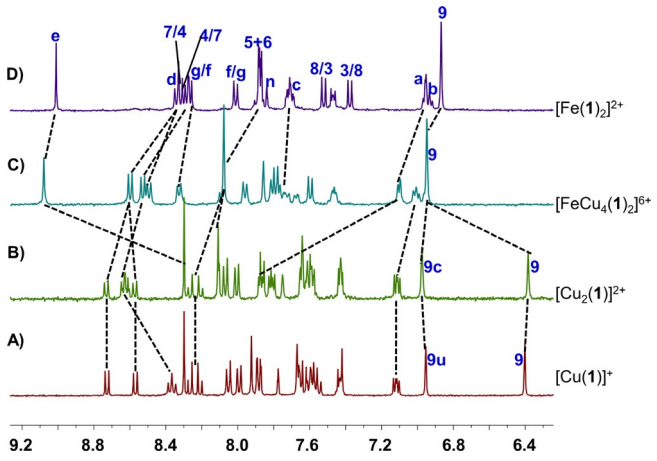

Figure 4. Partial ^{1}H NMR (400 MHz, 298 K) of (a) $[Cu(\mathbf{1})]^+$ in CD_2Cl_2 (State I$_1$); (b) $[(Cu_2(\mathbf{1})]^{2+}$ in CD_2Cl_2 (State II$_1$); (c) $[FeCu_4(\mathbf{1})_2]^{6+}$ in CD_2Cl_2:CD_3CN (5:1) (State III$_1$); (d) $[Fe(\mathbf{1})_2]^{2+}$ in CD_2Cl_2:CD_3CN (5:1) (State IV$_1$).

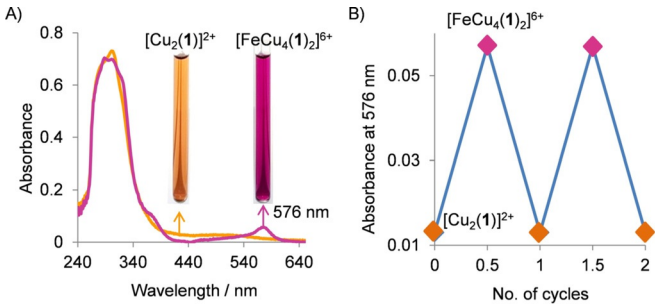

Figure 5. (A) UV-vis spectra and observable color of $[Cu_2(\mathbf{1})]^{2+}$ (1.25×10^{-4} M) and $[FeCu_4(\mathbf{1})_2]^{6+}$ (1.25×10^{-4} M) in CD_2Cl_2. (B) Two reversible switching cycles (between $[Cu_2(\mathbf{1})]^{2+}$ and $[FeCu_4(\mathbf{1})_2]^{6+}$) and changes in absorbance at $\lambda = 576$ nm.

biguously corroborated clean formation of the dimeric iron(II) terpyridine complex (Figure 4C). Further support for this assignment was received from the downfield shifted signal of the mesityl protons 9-H from 6.38 to 6.97 ppm that is characteristic for coordinatively frustrated $[Cu(phenAr_2)]^+$ complexes (Supporting Information, Figure S26). Additionally, ^{1}H-^{1}H COSY, ESI-MS, and elemental analysis verified the formation of the desired complex $[FeCu_4(\mathbf{1})_2]^{6+}$ (State III_1).

Then, copper(I) ions were removed to prepare $[Fe(\mathbf{1})_2]^{2+}$ (= State IV_1) by addition of 2.0 equiv of cyclam (with respect to **1**) as a strong chelating agent. In the ^{1}H NMR, the phenanthroline proton signal for 9c-H is upfield shifted to 6.87 ppm due to demetalation (Figure 4D; Supporting Information, Figure S28). The formation of complex $[Fe(\mathbf{1})_2]^{2+}$ was further evidenced by UV/vis, ^{1}H-^{1}H COSY, ESI-MS spectroscopy and elemental analysis. Finally, 0.5 equiv of hexacyclen was added to remove iron(II) and 1.0 equiv of copper(I) was added to go back to the initial state, State I_1. After the successful demonstration of the unidirectional cyclic switching along the states $I_1 \rightarrow II_1 \rightarrow III_1 \rightarrow IV_1 \rightarrow I_1$ (see Supporting Information, Figure S39) over two cycles, we verified the reversible switching between States II_1 and III_1 by UV/vis (Figure 5B) due to its importance for the ON/OFF-control of catalysis.

Since reversible toggling between States II_1 and III_1 was successful, the catalytic activity of the individual switching states was investigated. First, a mixture of nanoswitch **1** (3 mM in $CD_2Cl_2/CD_3CN = 5{:}1$, *v/v*), $[Cu(CH_3CN)_4]PF_6$, **A1** and **B** (1:2:10:10) representing State II_1 was heated (50 °C, 2 h). By ^{1}H NMR criteria, the acyl-transferred product **C1** was not formed (Supporting Information, Figure S47). As expected, blockage of one of the binding sites in $[Cu_2(\mathbf{1})]^{2+}$ by HETTAP complexation is sufficient to suppress acyl transfer. This finding suggested to regulate the reaction in an ON/OFF manner by unmasking/masking the copper(I)-loaded HETTAP site in $[Cu_2(\mathbf{1})]^{2+}$. Consequently, the ON state for acylation should be embodied by State III_1, where both the copper(I)-loaded phenanthrolines stations are available for catalysis. Thus, a mixture of **1** (3.0 mM), $[Fe(BF_4)_2]\cdot6H_2O$, $[Cu(CH_3CN)_4]PF_6$, **A1** and **B** (2:1:4:20:20) was tested for its catalytic action. As expected, State III_1 was catalytically active furnishing 33% of **C1** after 2 h of heating at 50 °C (Supporting Information, Figure S48).

After the concept of switchable proximity catalysis had been established for switch **1**, the larger nanoswitch **2** was prepared in order to extend the study toward multi-catalyst systems and their substrate selectivity. We selected a framework based on a tetrahedral core (Figure 6)[17] because there the distance between both copper(I)-loaded phenanthrolines is increased by 3.1 Å in comparison to that in switch **1** ($d = 14.9$ Å, see Supporting Information, chapter 8). Nanoswitch **2** was unambiguously characterized by spectral data (for its preparation and data, see the Supporting Information, Scheme S3). At first, we individually synthesized each of the switching States I_2, II_2, III_2 and IV_2 in pure form for characterization by ^{1}H, ^{1}H-^{1}H COSY, ESI-MS, and elemental analysis (Supporting Information). Secondly, we confirmed the clean in situ four-state switching (State $I_2 \rightarrow II_2 \rightarrow III_2 \rightarrow IV_2 \rightarrow I_2$) of **2** by alternate addition and removal of copper(I) and iron(II) ions (Supporting Information, Figure S40).

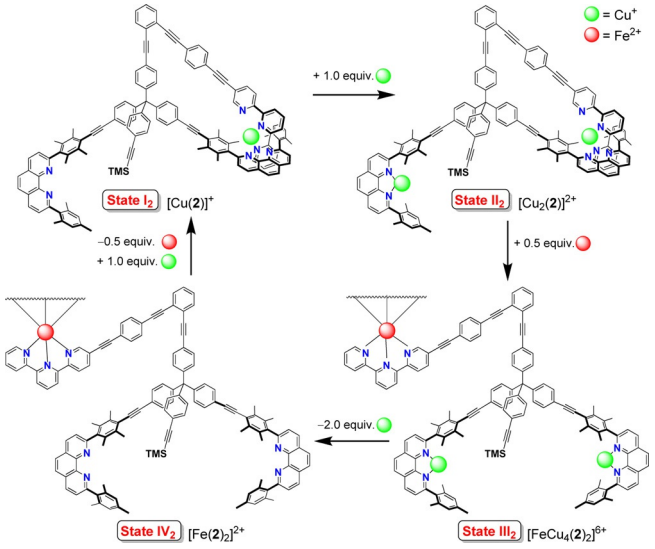

Figure 6. Four-state switching of nanoswitch **2** by addition/removal of copper(I) and iron(II) ions.

With nanoswitch **2** and its switching states being fully characterized, we investigated its ability to discriminate similar reactants by size. Markedly, neither State II_2 nor III_2 was able to noticeably catalyze the transformation of **A1**+**B**. Even in the presence of State III_2 (= $[FeCu_4(\mathbf{2})_2]^{6+}$; 5 mol%), where the copper(I) ions are exposed, the reaction (50 °C, 2 h) between **A1** (30.0 mM) and **B** (30.0 mM) gave only 2% of the product **C1** (Supporting Information, Figure S51). In contrast, a mix of switch **2** (3 mM), $[Fe(BF_4)_2]\cdot6H_2O$, $[Cu(CH_3CN)_4]PF_6$ (2:1:4) representing State III_2 plus the large alcohol **A2** & **B** (20:20) furnished 26% of product **C2** (Supporting Information, Figure S50). As expected, State $II_2 = [Cu_2(\mathbf{2})]^{2+}$ (10 mol%) was unable to promote any reaction between **A2** (30.0 mM) and **B** (30.0 mM) (Supporting Information, Figure S49).

For evaluating the larger alcohol in the smaller sized catalyst, we studied the reaction of **A2** and **B** in presence of model complex $[Cu_2(\mathbf{3})]^{2+}$. Since no formation of product **C2** was ob-

served at the same conditions (Supporting Information, Figure S52), we concluded that the substrate (4-(pyridin-4-yl)phenyl)methanol (**A2**) has an incompatible length with the cavity of $[Cu_2(\mathbf{3})]^{2+}$ that is equally part of $[FeCu_4(\mathbf{1})_2]^{6+}$ (State III_1 of switch **1**). This finding again clearly indicated that the dimensions of the substrates had a significant effect on catalysis and that preorganization of the substrate is not sufficient. In essence, a good fit of substrate and cavity dimensions is necessary to observe the proximity effect.

Statistically, three possible combinations of bound substrates (**A** and **A**, **A** and **B**, **B** and **B**) at both copper(I)-loaded phenanthrolines of $[Cu_2(\mathbf{3})]^{2+}$ are possible. Obviously only the hetero-combination of the reactants (**A** and **B**) will lead to increased reaction rates. To evaluate the coordination preferences of the substrates at the copper(I)-phenAr$_2$ sites, we mixed ligand **3** (3 mM), $[Cu(CH_3CN)_4]PF_6$, **A1** and **B** in 1:2:1:1 ratio and compared the results with those of the homo-combinations (1:2:2:0 and 1:2:0:2). All the pyridyl protons a-, b-, c-H and imidazole protons d-, e-, f-H in hetero-combination (1:2:1:1 mixture) were upfield shifted and became sharper in the ^{1}H NMR compared to those of the other two combinations (Supporting Information, Figure S41). We hypothesized that the hetero-combination of the substrates **A1** and **B** coordinated preferentially, better than the two homo arrangements (**A** & **A**, **B** & **B**). A possible reason for this binding preference is hydrogen bonding between the acetyl group of **B** and the hydroxyl group of **A1** that should lead to increased effective local concentrations. Moreover, the corresponding hemiacetal from **A** and **B**, although being a high energy intermediate, would fit perfectly into the cavity and thus could be responsible for the rate enhancement.

Next we individually evaluated the in situ ON/OFF control of proximity catalysis of the switches **1** (Figure 7A) and **2** (Figure 7B) by reversibly toggling between monomeric and dimeric states. Switching was accomplished by addition and removal of iron(II) ions.[18] A mixture of $[Cu_2(\mathbf{1})]^{2+}$ (3.00 mM), substrates pyridin-4-yl-methanol (**A1**) and 1-acetylimidazole (**B**) in 1:10:10 ratio in CD_2Cl_2:CD_3CN (5:1) was heated at 50 °C for 2 h. No acyl transfer was observed by ^{1}H NMR spectroscopy (Catalysis OFF in State II_1; Supporting Information, Figure S53a) which is readily justified on the basis of one blocked copper site. Upon addition of 0.5 equiv of $[Fe(BF_4)_2]\cdot 6H_2O$ (relative to **1**) to State II_1, complex $[FeCu_4(\mathbf{1})_2]^{6+}$ formed (State III_1). Heating of the reaction mixture at 50 °C for 2 h furnished the acylated product **C1** in 33% yield (Supporting Information, Figure S53b). Notably, the catalytic activity of $[FeCu_4(\mathbf{1})_2]^{6+}$ was similar as that of the catalytic reference system $[Cu_2(\mathbf{3})]^{2+}$.

After addition of consumed amounts of both substrates and 0.5 equiv of hexacyclen to remove iron(II) ions from the bis-homoleptic terpyridine complex, complex $[Cu_2(\mathbf{1})]^{2+}$ (State II_1) was furnished. The reaction mixture was again heated to 50 °C for 2 h. As expected, basically no increase in the acylated product **C1** was observed (Supporting Information, Figure S53c, total yield = 34%, increase in yield = 1%). A second cycle furnished similar catalytic activity (ON: 26%; OFF: 1%) reflecting a remarkable ON/OFF control (Figure 7C). Similarly, we also performed ON/OFF catalytic cycles for the acyl transfer between

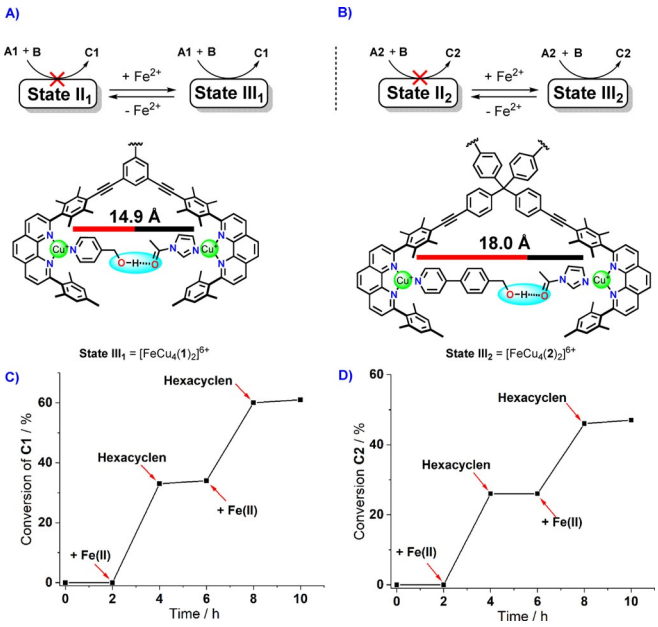

Figure 7. Representation of the ON/OFF regulation of the acyl transfer reaction by reversible switching between states III and II in both nanoswitches **1** (A and C) and **2** (B and D). (Consumed amounts of substrates were added each in step (after 2 h of heating)).

(4-(pyridin-4-yl)phenyl)methanol (**A2**) and **B** by toggling between $[Cu_2(\mathbf{2})]^{2+}$ (State II_2) and $[FeCu_4(\mathbf{2})_2]^{6+}$ (State III_2) (Supporting Information, Figure S54a-e). The reversibility of the system containing switch **2** was tested up to two cycles by addition and removal of iron(II) ions. In comparison with the catalytic cycles of switch **1**, similar results were observed for the formation of **C2**: ON1 = 26%, OFF1 = 0%, ON2 = 20%, OFF2 = 1% (Figure 7D; Supporting Information, Figure S54). Thus, both nanoswitches successfully controlled two consecutive catalytic cycles in an ON/OFF manner by opening/blocking one of the $[Cu(PhenAr_2)]^+$ binding sites. In the second cycle(s), a drop in the yield by 6–7% was observed, presumably due to the increasing concentration of coordinating species (product and generated by-product).

After the successful demonstration of catalytic cycles with both individual switches, we questioned whether selective opening of one cavity in a mixture containing both nanoswitches **1** and **2** would be possible. For that purpose, we first investigated the relative stability of $[Cu(\mathbf{1})]^+$ and $[Cu(\mathbf{2})]^+$. Upon addition of 1.0 equiv of $[Cu(CH_3CN)_4]PF_6$ to a 1:1 mixture of **1** and **2**, complex $[Cu(\mathbf{1})]^+$ formed quantitatively whereas **2** remained unaffected (Supporting Information, Figure S55). It clearly proved the superior stability of the copper(I)-HETTAP in $[Cu(\mathbf{1})]^+$ in comparison with that of $[Cu(\mathbf{2})]^+$.

On the basis of this finding, we envisioned that it should be possible to operate both nanoswitches as a 1:1 mixture and to selectively toggle the $[Cu(phenAr_2)]^+$-terpyridine bond in $[Cu_2(\mathbf{2})]^{2+}$. Indeed, upon adding 0.5 equiv of iron(II) ions to a 1:1 mixture of $[Cu_2(\mathbf{1})]^{2+}$ and $[Cu_2(\mathbf{2})]^{2+}$, the ^{1}H NMR confirmed the selective formation $[Cu_2(\mathbf{1})]^{2+}$ and $[FeCu_4(\mathbf{2})_2]^{6+}$ (Supporting Information, Figure S56). Addition of 0.5 equiv of hexacyclen selectively and immediately removed the iron(II) regener-

ating the initial mixture of $[Cu_2(\mathbf{1})]^{2+}$ and $[Cu_2(\mathbf{2})]^{2+}$ (Figure S56A). The selective and reversible activation of one nanoswitch in the presence of the other allowed the study of acyl transfer by opening $[Cu_2(\mathbf{2})]^{2+}$ in a mixture with $[Cu_2(\mathbf{1})]^{2+}$. Finally, the duo of nanoswitches **1** and **2** (both 3 mM), $[Fe(BF_4)_2]\cdot 6H_2O$, $[Cu(CH_3CN)_4]PF_6$, **A1**, **A2** and **B** (1:1:0.5:4:10:10:20) was heated in CD_2Cl_2:CD_3CN (5:1) at 50 °C. After 2 h, 17% of product **C2** and only 3% of **C1** were detected by ^{1}H NMR. Therefore, we were able to selectively activate nanoswitch $[Cu_2(\mathbf{2})]^{2+}$ in presence of $[Cu_2(\mathbf{1})]^{2+}$ thus achieving selective transformation in a catalyst duo (Supporting Information, Figure S58) and in a mixture of **A1**/ **A2**.

In conclusion, we have utilized two multistate nanoswitches, where one of the switching states (State III) showed increased catalytic activity due to two cooperatively[19] acting copper(I)-loaded phenanthroline sites. Binding of substrates at those sites leads to increased effective concentrations and higher reaction rates, whereas other states are inactive. In contrast, one of the copper(I) ions in State II is buried inside the HETTAP sites and thus unable to increase the rate of the acyl transfer reactions. Thus, reversible toggling back and forth between States III and II by addition/removal of 0.5 equiv of iron(II) ions leads to in situ ON/OFF regulation of the catalytic reaction. Finally, we demonstrated the selective actuation of one out of two nanoswitches in a mixture of all starting materials selectively leading to the formation of the product of the activated switch. We expect that the present work helps to understand and develop further switchable multi-catalyst systems that select between substrates of basically identical reactivity.[20]

Acknowledgements

We are grateful to the Deutsche Forschungsgemeinschaft (SCHM 647/19-2) and the University of Siegen for financial support. Open access funding enabled and organized by Projekt DEAL.

Conflict of interest

The authors declare no conflict of interest.

Keywords: allosteric regulation · molecular switches · multicomponent systems · proximity effects · switchable catalysis

[1] E. I. Solomon, U. M. Sundaram, T. E. Machonkin, *Chem. Rev.* **1996**, *96*, 2563 – 2606.
[2] A. Steven, W. Baumeister, L. N. Johnson, R. N. Perham, *Molecular Biology of Assemblies and Machines*, **2016**, Garland Science New York.
[3] a) N. Rad, O. Danylyuk, V. Sashuk, *Angew. Chem. Int. Ed.* **2019**, *58*, 11340 – 11343; *Angew. Chem.* **2019**, *131*, 11462 – 11465; b) M. Dommaschk, J. Echavarren, D. A. Leigh, V. Marcos, T. A. Singleton, *Angew. Chem. Int. Ed.* **2019**, *58*, 14955 – 14958; *Angew. Chem.* **2019**, *131*, 15097 – 15100; c) C. Z.-J. Ren, P. Solís Muñana, J. Dupont, S. S. Zhou, J. L.-Y. Chen, *Angew. Chem. Int. Ed.* **2019**, *58*, 15254 – 15258; *Angew. Chem.* **2019**, *131*, 15398 – 15402; d) R. Dorel, B. L. Feringa, *Angew. Chem. Int. Ed.* **2020**, *59*, 785 – 789; *Angew. Chem.* **2020**, *132*, 795 – 799.
[4] Recent reviews on Switchable Catalysis a) M. Raynal, P. Ballester, A. Vidal-Ferran, P. W. N. M. van Leeuwen, *Chem. Soc. Rev.* **2014**, *43*, 1660 – 1733; and b) M. Raynal, P. Ballester, A. Vidal-Ferran, P. W. N. M. van Leeuwen, *Chem. Soc. Rev.* **2014**, *43*, 1734 – 1787; c) D. A. Leigh, V. Marcos, M. R. Wilson, *ACS Catal.* **2014**, *4*, 4490 – 4497; d) V. Blanco, D. A. Leigh, V. Marcos, *Chem. Soc. Rev.* **2015**, *44*, 5341 – 5370; e) A. J. McConnell, C. S. Wood, P. P. Neelakandan, J. R. Nitschke, *Chem. Rev.* **2015**, *115*, 7729 – 7793; f) M. Vlatković, B. S. L. Collins, B. L. Feringa, *Chem. Eur. J.* **2016**, *22*, 17080 – 17111; g) L. van Dijk, M. J. Tilby, R. Szpera, O. A. Smith, H. A. P. Bunce, S. P. Fletcher, *Nat. Rev. Chem.* **2018**, *2*, 0117; h) A. Goswami, S. Saha, P. K. Biswas, M. Schmittel, *Chem. Rev.* **2020**, *120*, 125 – 199.
[5] a) J.-M. Lehn, *Angew. Chem. Int. Ed.* **2013**, *52*, 2836 – 2850; *Angew. Chem.* **2013**, *125*, 2906 – 2921; b) M. Schmittel, *Chem. Commun.* **2015**, *51*, 14956 – 14968; c) J.-F. Ayme, J.-M. Lehn, *Adv. Inorg. Chem.* **2018**, *71*, 3 – 78; d) B. J. Cafferty, A. S. Ten, M. J. Fink, S. Morey, D. J. Preston, M. Mrksich, G. M. Whitesides, *ACS Cent. Sci.* **2019**, *5*, 911 – 916.
[6] a) H. J. Yoon, J. Heo, C. A. Mirkin, *J. Am. Chem. Soc.* **2007**, *129*, 14182 – 14183; b) M. Samanta, V. S. Rama Krishna, S. Bandyopadhyay, *Chem. Commun.* **2014**, *50*, 10577 – 10579.
[7] a) J. Wang, B. L. Feringa, *Science* **2011**, *331*, 1429 – 1432; b) S. Mortezaei, N. R. Catarineu, J. W. Canary, *J. Am. Chem. Soc.* **2012**, *134*, 8054 – 8057; c) D. Zhao, T. M. Neubauer, B. L. Feringa, *Nat. Commun.* **2015**, *6*, 6652.
[8] a) F. Würthner, J. Rebek, *Angew. Chem. Int. Ed. Engl.* **1995**, *34*, 446 – 448; *Angew. Chem.* **1995**, *107*, 503 – 505; b) I. O. Fritsky, R. Ott, R. Krämer, *Angew. Chem. Int. Ed.* **2000**, *39*, 3255 – 3258; *Angew. Chem.* **2000**, *112*, 3403 – 3406; c) R. Cacciapaglia, S. Stefano, L. Mandolini, *J. Am. Chem. Soc.* **2003**, *125*, 2224 – 2227; d) T. Imahori, R. Yamaguchi, S. Kurihara, *Chem. Eur. J.* **2012**, *18*, 10802 – 10807; e) L. Benda, B. Doistau, C. Rossi-Gendron, L.-M. Chamoreau, B. Hasenknopf, G. Vives, *Commun. Chem.* **2019**, *2*, 144.
[9] S. Hederos, L. Baltzer, *Biopolymers* **2005**, *79*, 292 – 299.
[10] a) C. G. Oliveri, N. C. Gianneschi, S. T. Nguyen, C. A. Mirkin, C. L. Stern, Z. Wawrzak, M. Pink, *J. Am. Chem. Soc.* **2006**, *128*, 16286 – 16296; b) M. J. Wiester, P. A. Ulmann, C. A. Mirkin, *Angew. Chem. Int. Ed.* **2011**, *50*, 114 – 137; *Angew. Chem.* **2011**, *123*, 118 – 142; c) H. F. Cheng, A. I. d'Aquino, J. Barroso-Flores, C. A. Mirkin, *J. Am. Chem. Soc.* **2018**, *140*, 14590 – 14594.
[11] L. G. Mackay, R. S. Wylie, J. K. M. Sanders, *J. Am. Chem. Soc.* **1994**, *116*, 3141 – 3142.
[12] S. De, K. Mahata, M. Schmittel, *Chem. Soc. Rev.* **2010**, *39*, 1555 – 1575.
[13] M. L. Saha, S. Neogi, M. Schmittel, *Dalton Trans.* **2014**, *43*, 3815 – 3834.
[14] S. De, S. Pramanik, M. Schmittel, *Dalton Trans.* **2014**, *43*, 10977 – 10982.
[15] A. Goswami, M. Schmittel, *Angew. Chem. Int. Ed.* **2020**, *59*, 12362 – 12366; *Angew. Chem.* **2020**, *132*, 12461 – 12465.
[16] S. Gaikwad, A. Goswami, S. De, M. Schmittel, *Angew. Chem. Int. Ed.* **2016**, *55*, 10512 – 10517; *Angew. Chem.* **2016**, *128*, 10668 – 10673.
[17] a) S. Gaikwad, M. Schmittel, *J. Org. Chem.* **2017**, *82*, 343 – 352; b) S. Gaikwad, S. Pramanik, S. De, M. Schmittel, *Dalton Trans.* **2018**, *47*, 1786 – 1790; c) S. Gaikwad, M. S. Özer, S. Pramanik, M. Schmittel, *Org. Biomol. Chem.* **2019**, *17*, 7956 – 7963.
[18] For nanoswitch **1** and **2** we used **A1** and **A2** respectively due to their suitable length.
[19] a) C. Kremer, A. Lützen, *Chem. Eur. J.* **2013**, *19*, 6162 – 6196; b) G. H. Clever, P. Punt, *Acc. Chem. Res.* **2017**, *50*, 2233 – 2243.
[20] L. Falivene, Z. Cao, A. Petta, L. Serra, A. Poater, R. Oliva, V. Scarano, L. Cavallo, *Nat. Chem.* **2019**, *11*, 872 – 879.

Manuscript received: October 1, 2020
Accepted manuscript online: October 6, 2020
Version of record online: January 18, 2021